



# A Plasma Algorithm for Plasmoid Accelerator Modeling

**John Loverich and Jean-Luc Cambier**

Advatech Pacific and AFRL Edwards

APS Division of Plasma Physics

Philadelphia, Pennsylvania, October 30 - November 4, 2006

URL <http://www.advatechpacific.com>

email: [john.loverich@advatechpacific.com](mailto:john.loverich@advatechpacific.com)



## Abstract

In this paper we present discontinuous Galerkin approaches to resistive/ideal MHD and Hall MHD plasma models. A correction potential approach and a constrained transport approach using vector potentials are implemented to minimize  $\nabla \cdot B$  errors. The algorithms work in axisymmetric and general geometries and are tested on applications relevant to plasmoid accelerator modeling. Simple FRC formation and acceleration simulations are presented along with various benchmarks.



## Resistive Hall MHD

A total continuity equation is used,

$$\frac{\partial \rho}{\partial t} + \nabla \cdot [\rho U] = 0, \quad (1)$$

Along with a total momentum equation,

$$\frac{\partial \rho U}{\partial t} + \nabla \cdot \left[ \rho U U + P - \frac{1}{\mu_0} B B + \frac{1}{2 \mu_0} B \cdot B \right] = 0, \quad (2)$$

an ion energy equation,

$$\frac{\partial e}{\partial t} + \nabla \cdot \left[ U \left( e + P + \frac{1}{2 \mu_0} B \cdot B - \frac{1}{\mu_0} (B \cdot U) B + \frac{1}{\mu_0} \eta J \times B \right) \right] = 0. \quad (3)$$

Reduced electron momentum equation, i.e., Ohm's law is

$$E = -U \times B + \frac{J}{n q} \times B + \eta J. \quad (4)$$

The magnetic induction equation is also included

$$\frac{\partial B}{\partial t} + \nabla \times E = 0. \quad (5)$$



## Dealing With Divergence Errors - relaxation

The first technique applied is hyperbolic divergence cleaning with relaxation. This is related to parabolic divergence cleaning in that it is the hyperbolic approximation of parabolic divergence cleaning. The magnetic field equation with parabolic divergence cleaning is written,

$$\frac{\partial B}{\partial t} + \nabla \times E = \Gamma_2 \nabla (\nabla \cdot B) \quad (6)$$

the diffusive term has a time step restriction that goes like  $\Delta x^2$ , but this problem is eliminated by moving to a hyperbolic approximation of the diffusion equation. This produces the hyperbolic divergence cleaning technique with relaxation as developed by Dedner[2]

$$\frac{\partial B}{\partial t} + \nabla \times E + \nabla \phi = 0 \quad (7)$$

$$\frac{\partial \phi}{\partial t} + \Gamma_1^2 \nabla \cdot B = -\Gamma_2 \phi. \quad (8)$$



## Dealing With Divergence Errors - Vector Potential

Another approach that is particularly well suited to the discontinuous Galerkin method is solving the vector potential equation, thus

$$\frac{\partial A}{\partial t} + E = 0, \quad (9)$$

$$B = \nabla \times A. \quad (10)$$

This technique has been found to work well for problems with dynamic boundary conditions such as those produced by electromagnetic coils. The correction potential approach performs poorly for these same types of problems. In the discontinuous Galerkin method both the magnetic field and the vector potential are cell centered, furthermore, boundary conditions on the vector potential are easy to apply - the time dependent vector potential equation is simply evaluated in the ghost cells. The technique looks virtually identical to constrained transport methods that are sometimes used in finite volume methods.



## Dispersion Relation

It's helpful to examine the waves of the system to help understand the numerical limitations imposed by them. Starting with a uniform background plasma, we assume a small perturbation from uniform equilibrium and derive the following dispersion relations for the linearized solution. Define  $V_a = \sqrt{\frac{B_0^2}{m_i n_i \mu_0}}$  and  $V_w = \frac{B_0}{2e n_0 \mu_0}$ , and

$V_s = \sqrt{\frac{\gamma P}{m_i n_0}}$  then in the parallel case we have,

$$\omega = \pm V_w k^2 \pm \sqrt{V_a k^2 + V_w k^4} \quad (11)$$

$$\omega = \pm V_s k \quad (12)$$

and in the perpendicular case we have,

$$\omega = \pm \sqrt{V_s^2 + V_a^2} k . \quad (13)$$

Note that the dispersion relations 14,12,13 are different from the characteristic wave speeds calculated for Riemann solvers in that the background fluid velocity was set to 0 and these waves only apply for direction perpendicular and parallel to the magnetic field. The important point is that the whistler wave, equation 14 is quadratic in  $k$  so the wave



speed increases with the wave number. This fact is problematic for explicit numerical methods because it means the time step goes as  $\Delta x^2$  instead of  $\Delta x$ . In the limit of large  $k$ , equation 14 becomes,

$$\omega = \pm 2 V_w k^2 . \quad (14)$$

This quadratic dispersion relation is identical to the dispersion relation for the Schrodinger equation. With that in mind, an appropriate model problem for hall MHD is the Schrodinger equation and we can borrow numerical techniques developed for that system. Fortunately, the discontinuous Galerkin method has already been applied to the Schrodinger equation so we can apply those same lessons to the Hall MHD system.



## Discontinuous Galerkin Method

The systems of equations described consist of balance laws with auxiliary variables. One benefit of the discontinuous Galerkin method over finite volume methods is that it's straight forward to apply to systems that are not written in divergence form.

We consider two types of equations, one is a balance law written in divergence form, the other is an auxiliary equation. The balance law is written,

$$\frac{\partial Q_c}{\partial t} + \nabla \cdot F_c(Q_c, Q_a) = \psi(Q_c, Q_a) + g_c(r, Q_c, Q_a) . \quad (15)$$

The auxiliary equation is written,

$$Q_a + \nabla \cdot F_a(Q_c) = g_a(r, Q_c) , \quad (16)$$

where  $g$  are geometric source terms used when the code is run in axisymmetric geometries.



## Discontinuous Galerkin Method

The equation is written,

$$\begin{aligned} \int \frac{\partial Q_c}{\partial t} v_r dV + \int (\nabla \cdot F_c) v_r dV &= \int \psi v_r dV \\ \int Q_a v_r dV + \int (\nabla \cdot F_a) v_r dV &= 0. \end{aligned} \quad (17)$$

Integration by parts yields

$$\begin{aligned} \int_K \frac{\partial Q}{\partial t} v_r dV + \int_{\partial K} (F \cdot n) v_r d\Gamma - \int_K F \cdot (\nabla v_r) dV &= \int \psi v_r dV \\ \int_K Q_a v_r dV + \int_{\partial K} (F \cdot n) v_r d\Gamma - \int_K F \cdot (\nabla v_r) dV &= 0. \end{aligned} \quad (18)$$

The discrete conserved variable  $q$  is defined as a linear combination of the basis functions inside an element  $K$ , with

$$Q = \sum_r v_r Q_r. \quad (19)$$

Runge-Kutta time integration is used to evaluate the time derivatives[1] and Gaussian Quadrature is used to evaluate the volume and surface integrals. Notice that we have some freedom in choosing the surface flux because the solution is discontinuous at surfaces. At the surfaces a numerical flux function is defined and is discussed later.



## Numerical Flux Functions - Balance Equations

For the balance equations the numerical flux is calculated using a Lax flux or an HLL flux

$$\tilde{F}_{i+\frac{1}{2}} = \frac{1}{2} (F_i^+ + F_{i+1}^-) - |\lambda| (Q_i^+ - Q_{i+1}^-) . \quad (20)$$

If hyperbolic divergence cleaning is used then a different diffusion coefficient  $\lambda$  can be used for the correction potential equation to reduce excessive diffusion in the remaining equations where the characteristic wave speeds are smaller.



## Numerical Flux Functions - Auxiliary Equations

In the auxiliary equations the flux can be calculated using a centered difference,

$$\tilde{F}_{i+\frac{1}{2}} = \frac{1}{2} (F_i^+ + F_{i+1}^-) . \quad (21)$$

No diffusion term is required for these equations. A HLL flux ignoring the diffusion term can also be used; this amounts to providing a weighted average of each flux that depends on the minimum and maximum Eigen values at the interface. Limiters can be applied to the auxiliary variables in exactly the same way they are applied to the conserved variables. In the case of the correction potential approach the auxiliary variable and equation is  $J = \frac{1}{\mu_0} \nabla \times B$  and in the case of the vector potential approach the auxiliary variables and equations are  $B = \nabla \times A$  and  $J = \frac{1}{\mu_0} \nabla \times B$ .



## Brio and Wu Shock

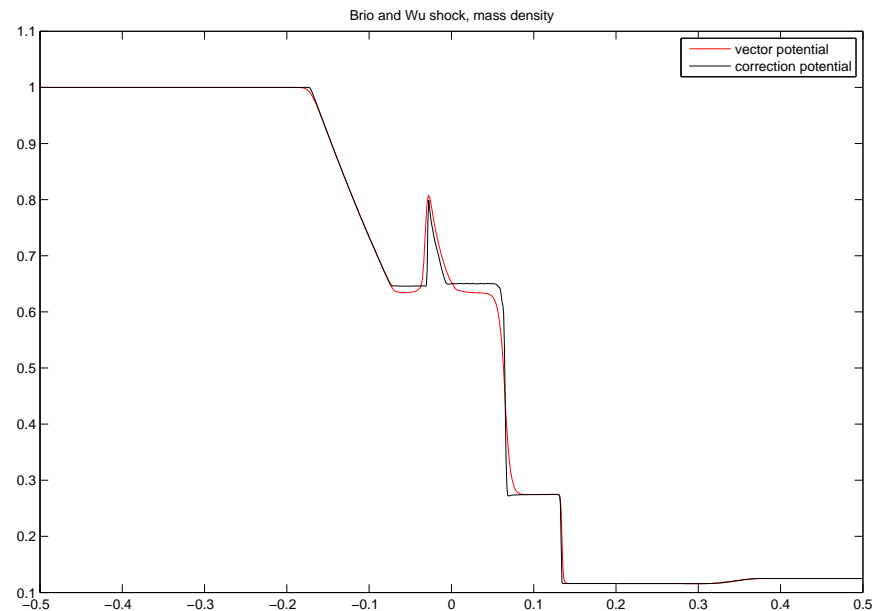


Figure 1: This problem is a test of the shock capturing ability of the two methods. The correction potential approach works considerably better in this type of problem though there may be techniques we can apply to improve the vector potential solution. Note that in this 1D problem, divergence errors do not occur so they do not pollute the solution.



## Shock Bubble Interaction - Ideal MHD

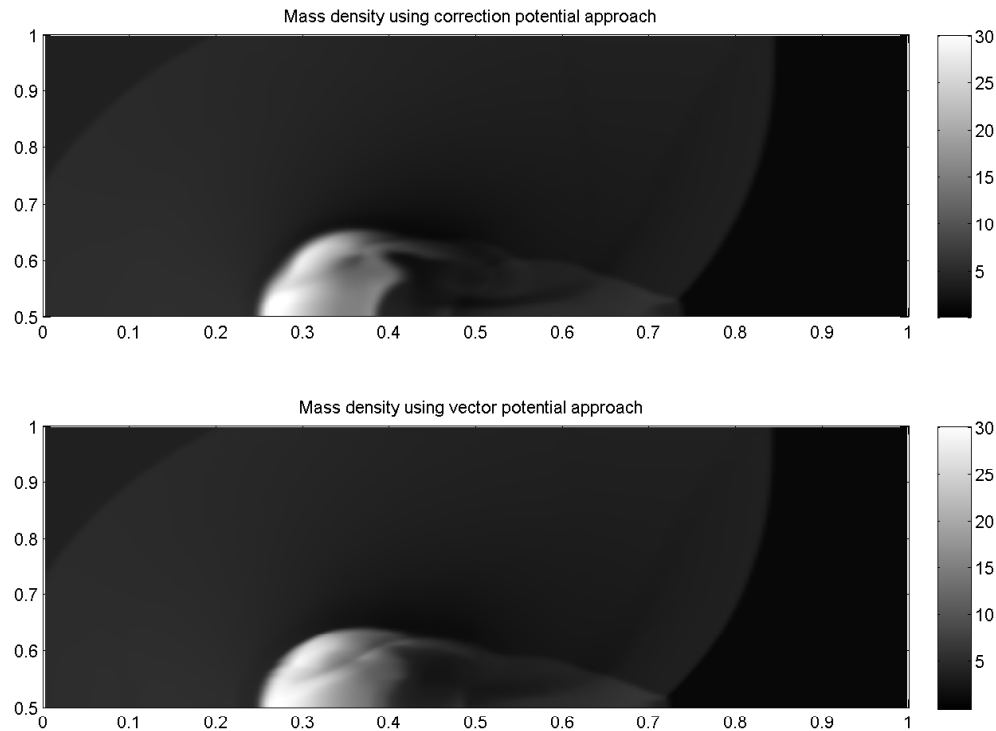


Figure 2: Solution to the shock bubble interaction problem of Toth[3]. This problem is a good test of shock capturing ability of numerical MHD codes. It is seen that the vector potential algorithm is more diffusive than the correction potential algorithm in this 2 dimensional problem with in plane magnetic fields. These results agree well with published results.



## Collisionless Reconnection

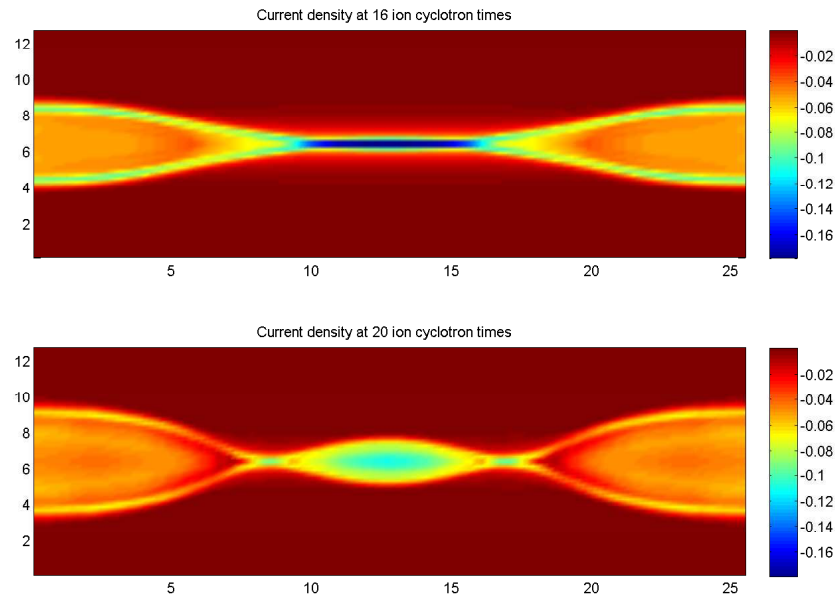


Figure 3: Plot of  $z$  current density in the GEM challenge magnetic reconnection problem using the correction potential Hall MHD code. The results are shown at two times, one before the formation of a magnetic island and one after the formation. Magnetic islands increase the reconnection rate which then returns to normal when the island merges with one of the lobes. Unfortunately, we have not yet produced a scheme with the vector potential approach that is stable when the Hall term is included so the two techniques cannot be compared on this problem.



## FRC formation and acceleration - vector potential

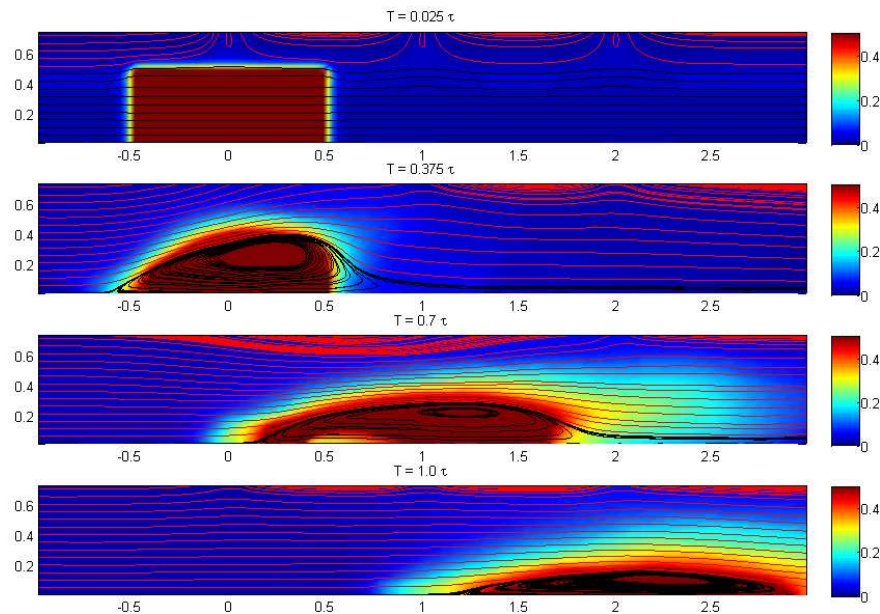


Figure 4: These plots show FRC formation and acceleration. Currently, formation occurs through magnetic diffusion around a high conductivity blob of plasma. Coils on the boundaries are pulsed in sequence to accelerate the FRC out of the domain. In this high inertia FRC, a significant part of the plasma diffuses across the separatrix.



## FRC formation and acceleration - vector potential

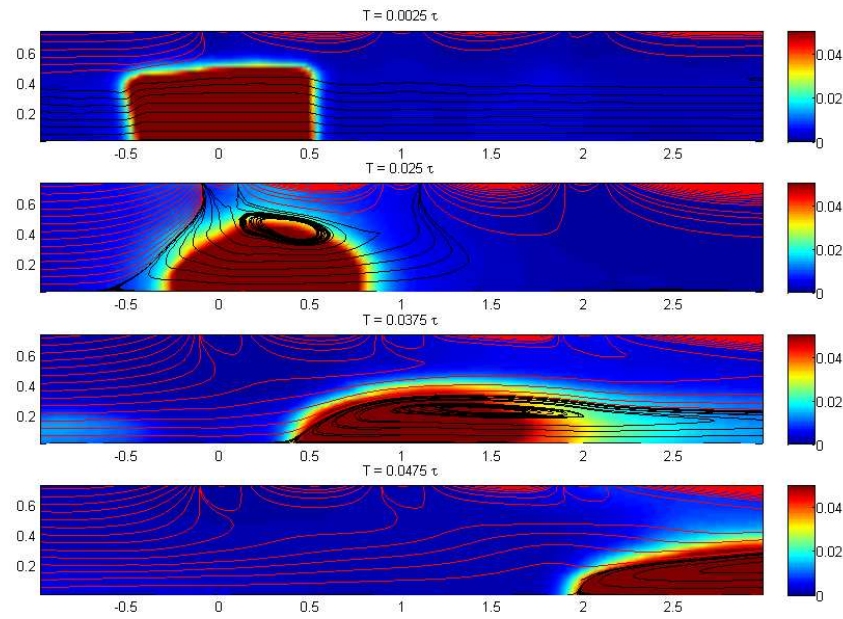


Figure 5: These plots show FRC formation and acceleration. In this case a much lower density plasma is generated and the plasmoid accelerates out of the domain before the second coil is pulsed and before the FRC is fully formed.



## Conclusion

Two algorithms using the discontinuous Galerkin method are currently in development for application to FRC thruster modeling. Though the correction potential method has many of the desirable properties of shock capturing schemes it does not perform well in the presence of dynamic boundary conditions where divergence errors can be quite large. A better solution to the problem of dynamic boundary conditions is the vector potential approach. However, the discontinuous Galerkin method applied to the vector potential problem does not yet stand on a firm theoretical footing and considerable improvements could be made. The Hall term works properly for the correction potential algorithm, but appears to be unstable in the case of the vector potential solutions. The issues with the Hall term in the vector potential algorithm are still under investigation.



# References



- [1] Bernardo Cockburn and Chi-Wang Shu, *Tvb runge-kutta local projection discontinuous galerkin finite element method for conservation laws ii: General framework*, Mathematics of Computation **52** (1989), 411–435.
- [2] A. Dedner, F. Kemm, D. Kroner, T. Schnitzer, and M. Wesenberg, *Hyperbolic divergence cleaning for the mhd equations*, Journal of Computational Physics **175** (2002), 645–673.
- [3] Gabor Toth, *The divb constraint in shock-capturing magnetohydrodynamics codes*, Journal Of Computational Physics **161** (2000), 605–652.